

Advanced fast marching tractography based on SENSE-DTI: An attempt to resolve fiber crossing in artificial and in-vivo data

P. Staempfli^{1,2}, T. Jaermann^{1,2}, G. R. Crelier¹, D. Meier¹, A. Valavanis², S. Kollias², P. Boesiger¹

¹Institute for Biomedical Engineering, University and ETH Zurich, CH-8092 Zurich, Switzerland, ²Institute of Neuroradiology, University Hospital Zurich, CH-8092 Zurich, Switzerland

Introduction

Fiber Tractography based on DTI data (for a review, see [1]) is extremely sensitive to the uncertainty of the main diffusion direction [2]. The reason for this is the voxel-averaged nature of the diffusion tensor: Fiber structures are much smaller than the resolution of DTI datasets, therefore, only the superimposed averaged diffusion direction of all fiber structures inside a voxel is dominant [2, 3]. Consequently, tracking algorithms incorporating only the main eigenvector for determining the propagation direction are not adequate for regions with crossing fiber pathways and often fail in such situations. This is a key obstacle for fiber tractography based on DTI data.

The fast-marching (FM) technique [4] is a promising approach to perform fiber tracking. Until now, only FM algorithms considering the main diffusion eigenvectors have been investigated [5, 6]. In this study, an advanced implementation of FM is proposed. It is hypothesized that the advanced FM algorithm alleviates the problem of reconstructing trajectories in brain regions where fiber systems intersect. For validation purpose, the algorithm is applied both to artificial diffusion data as well as to in-vivo data. Finally, the results are compared to the outcome of the basic FM and the well established FACT line propagation algorithm [7].

Methods

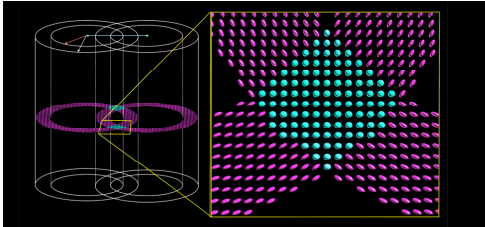


Fig.1: Artificial dataset of two intersecting cylinders to simulate crossing situations. On the right side, a zoomed view of the crossing section is depicted. (Note the planar shaped diffusion ellipsoids in the intersection region.)

Artificial diffusion data were created using the following geometric parameters: 128x128x46 voxels, in-plane resolution=1.6x1.6mm, slice thickness=2mm. Each voxel contained three orthogonal vectors and three eigenvalues, representing the corresponding diffusion properties. The data consisted of two intersecting cylinders to imitate different crossing and branching situations (Fig.1). The cylinders were mathematically superimposed, resulting in planar shaped diffusion ellipsoids in regions with fiber intersections. In such crossing areas the main eigenvectors are the result of the superposition of the individual diffusion tensors and do no longer point into any of the individual diffusion directions.

In-vivo data from healthy volunteers were acquired using a 3 T whole body system (Philips Medical Systems) equipped with 80mT/m/ms gradient coils and an 8-element receive head coil array (MRI Devices Corp.). A sensitivity encoding (SENSE) [8] factor of 2.1 was applied in a diffusion-weighted single-shot spin-echo EPI sequence. Diffusion weighting with a b -factor of 1000s/mm² was carried out along 15 directions, complemented by one scan with $b=0$. The geometric parameters were chosen as in the artificial data (FOV=200x200mm², matrix=128x128, 46 contiguous slices, slice thickness=2.0mm).

The advanced FM-algorithm which deploys the advantages of classical FM introduces a diffusion ellipsoid shape dependent propagation of the tracking front. For this purpose the algorithm takes into account the entire

diffusion tensor information. The voxels are subdivided into three classes, depending on the diffusion ellipsoid's shape. After classification into linear, planar and spherical diffusion distributions, each voxel group is assigned a specific front evolution velocity function v . These velocity functions are based on the idea of the tensor deflection approach [9].

The advanced FM algorithm was applied to the artificial datasets (Fig.2) as well as to the in-vivo data (Fig.3) and compared to the basic FM and the FACT algorithm. For the in-vivo comparison, the commissural system of the Corpus Callosum (CC) was chosen. It penetrates the Corona Radiata, an area where the radiation of the CC and axons of the projection system intersect. The commissural system was reconstructed using a seed area in a sagittal slice covering the center of the CC.

Results

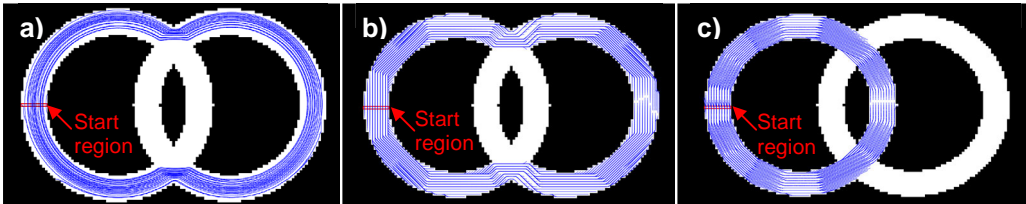


Fig.2: Crossing situation: Fibers (blue) are generated with different tracking algorithms from the same start region (red arrow). From left to right: FACT algorithm (a), basic FM algorithm (b), advanced FM algorithm (c).

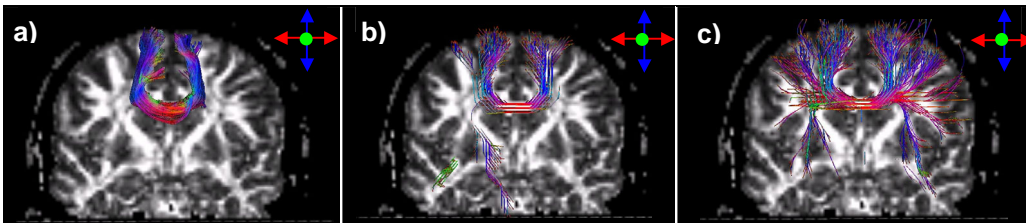


Fig.3: Reconstructed, directionally color coded fibers from a start region in the Corpus Callosum with the FACT (a), the basic FM (b) and the advanced FM (c) algorithm.

Fig.2 shows the resulting pathways of the FACT (Fig.2a), basic FM (Fig.2b) and the advanced FM algorithm (Fig.2c) in a planar section of the artificial data, in which a 90 degree intersection situation was simulated. Despite fiber crossing, the advanced FM algorithm reconstructs all pathways correctly. The trajectories of the FACT and the basic FM algorithm are deviated into the second cylinder.

The resulting tracks of the radiation of the CC (Fig.3) show the diversity of the three algorithms: The pathways of the advanced FM algorithm (Fig.3c) penetrate large parts of the hemisphere, in general agreement with known anatomy. In comparison, the resulting tracks of the FACT (Fig.3a) and the basic FM algorithm (Fig.3b) are deviated into the area of the Corona Radiata, where the CC radiation intersects the projection system.

Discussion and Conclusion

DTI based tractography is a powerful technique to investigate white matter anatomy and disease in vivo and non-invasively. The results of this study demonstrate the superior performance of the advanced FM algorithm in situations with crossing fibers compared to the original FM or FACT algorithms. The advanced FM algorithm is able to reconstruct fiber structures that are in good agreement with known white matter anatomy.

References

- [1] Mori S, et al. NMR in Biomed. 2002;15:468-480. [2] Jones DK, Magn Reson Med 2003;49:7-12. [3] Barrick TR, et al. Neuroimage 2004;22:481-491. [4] Sethian JA, Proc Natl Acad Sci USA 1996;93:1591-1595. [5] Parker GJM, et al. IEEE Trans Med Imag. 2002;21:505-512. [6] Parker GJM, et al. Neuroimage 2002;15:797-809. [7] Mori S, et al. Ann Neurol 1999;45:265-269. [8] Pruessmann KP, et al. Magn Reson Med 1999; 42: 952-962. [9] Lazar M, et al. Human Brain Mapping 2003;18:306-321.